226523: biotite–muscovite granodiorite gneiss, Rose Bore

(Rose Bore Granite, Tickalara Metamorphics, Central Zone, Lamboo Province, Halls Creek Orogen)

Location and sampling

Dixon Range (SE 52-6), Mcintosh (4462)
MGA Zone 52, 374924E 8031673N

Sampled on 16 July 2017

This sample was collected from outcrop in the bed of the Upper Panton River on Alice Downs Station, about 7.6 km southwest of Queensland Creek Bore, 4.5 km north-northeast of Nellies Spring Bore, and 2.6 km southeast of Rose Bore.

Tectonic unit/relations

The unit sampled is the Rose Bore Granite of the Tickalara Metamorphics. The Tickalara Metamorphics is the oldest rock unit recognized in the Central Zone of the Lamboo Province, and includes all the mafic metavolcanic, metasedimentary, and metagranitic rocks in the Central Zone that were deformed and metamorphosed during the first tectonothermal event (D_1/M_1) of the Hooper Orogeny (Tyler and Phillips, 2019b). The Rose Bore Granite consists of foliated, locally migmatitic, biotite–muscovite metagranitic rocks and felsic gneiss (Tyler et al., 1997; Tyler and Phillips, 2019a). At this locality, the rock is quartz-rich and exhibits a strong, variably sheared gneissic fabric deformed by upright, north-northwesterly trending folds and overprinted by small leucosome patches (Fig. 1). Previous U–Pb zircon dating of the Rose Bore Granite yielded a date of 1863 ± 3 Ma, interpreted as the magmatic crystallization age and a minimum depositional age for the sedimentary precursor of the pelitic gneiss that it intrudes (GA 113439, Page and Hoatson, 2000). A minimum age for the Rose Bore Granite is provided by a crosscutting Panton Suite intrusion, dated at 1853 ± 2 Ma (GA 93526033, Page and Hoatson, 2000). About 1.1 km to the northeast, a muscovite-bearing pegmatite that cuts the Panton intrusion yielded an igneous crystallization age of 1825 ± 10 Ma (GA 93526031, Page and Hoatson, 2000).

Petrographic description

The sample is a strongly foliated, biotite–muscovite granodiorite gneiss (Fig. 1), consisting of about 35% quartz, 35% plagioclase, 15% K-feldspar, 10% biotite, 5% muscovite, and accessory magnetite and zircon. Quartz is anhedral, up to 1.5 mm in size, weakly to moderately undulose, and partly in aggregates or in elongate quartz lenses or augen up to 8 mm long. Plagioclase is anhedral, equant to elongate, up to 2 mm in size, and mainly distinguished by sericite alteration. Some plagioclase grains exhibit tapered deformation twins. K-feldspar is mainly anhedral, microperthitic, up to 1.5 mm in size, with patches showing microcline twinning. Brown biotite forms subhedral laths up to 1.7 mm long, mainly in semi-aligned aggregates forming semi-continuous folia. Muscovite occurs as subhedral laths, in part with cleavage parallel to that in adjacent biotite, but also with cleavage orthogonal to the foliation. Bladed magnetite is up to 0.3 mm long, and mainly parallel to cleavage within micas. The strong tectonic foliation defined by the two micas is slightly warped across incipient shear planes. Deformation probably occurred at low to moderate grade (biotite facies).

Zircon morphology

Zircons isolated from this sample are colourless to dark brown, and subhedral to anhedral. The crystals are up to 200 μm long, and equant to elongate, with aspect ratios up to 4:1. In cathodoluminescence (CL) images, concentric zoning is ubiquitous. A CL image of all zircons is shown in Figure 2.

Analytical details

This sample was analysed on 19–20 and 22 October 2018, using SHRIMP-B. Analyses 1.1 to 20.1 (spot numbers 1–20) were obtained during the first session, together with 10 analyses of the M257 standard, of which five analyses indicated an external spot-to-spot (reproducibility) uncertainty of 0.50% (1σ) and a $^{238}U/^{206}Pb^*$ calibration uncertainty of 0.28% (1σ). Analyses 21.1 to 27.1 (spot numbers 21–27) were obtained during the second session, together with eight analyses of the M257 standard, of which seven analyses indicated an external spot-to-spot (reproducibility) uncertainty of 0.50% (1σ) and a $^{238}U/^{206}Pb^*$ calibration uncertainty of 0.23% (1σ). Calibration uncertainties are included in the errors of $^{238}U/^{206}Pb^*$ ratios and dates listed in Table 1. Common-Pb corrections were applied to all analyses using contemporaneous isotopic compositions determined according to the model of Stacey and Kramers (1975).

Results

Twenty-seven analyses were obtained from 27 zircons. Results are listed in Table 1, and shown in a concordia diagram (Fig. 3).

Figure 1. **Outcrop image for sample 226523: biotite–muscovite granodiorite gneiss, Rose Bore**

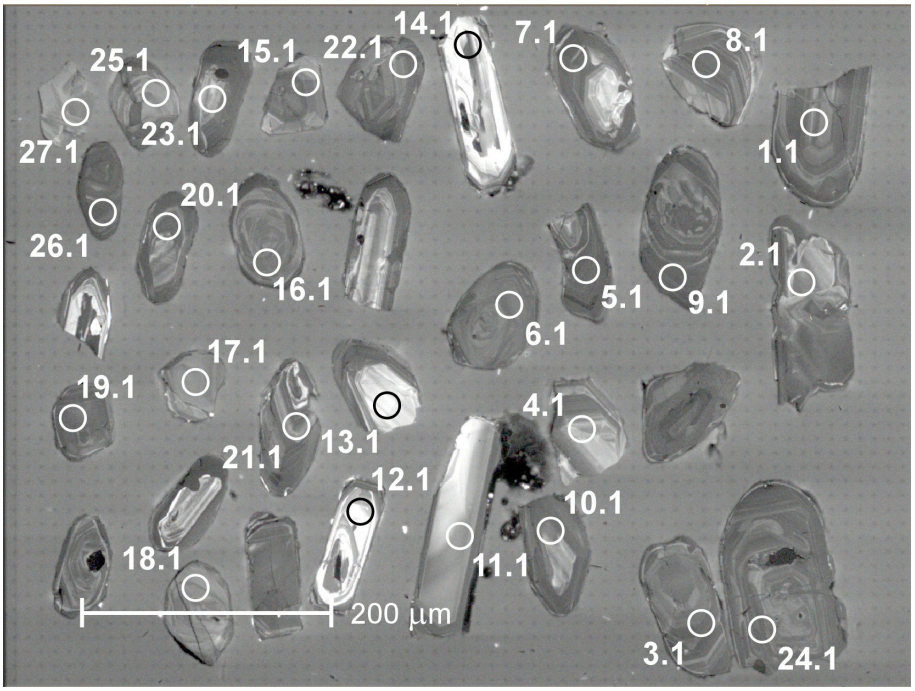

Figure 2. **Cathodoluminescence image of all zircons from sample 226523: biotite–muscovite granodiorite gneiss, Rose Bore. Numbered circles indicate the approximate locations of analysis sites**

Table 1. Ion microprobe analytical results for zircons from sample 226523: biotite–muscovite granodiorite gneiss, Rose Bore

Group ID	Spot no.	Grain. spot	^{238}U (ppm)	^{232}Th (ppm)	$\frac{^{232}Th}{^{238}U}$	f204 (%)	$^{238}U/^{206}Pb$ ± 1σ		$^{207}Pb/^{206}Pb$ ± 1σ		$^{238}U/^{206}Pb^*$ ± 1σ		$^{207}Pb^*/^{206}Pb^*$ ± 1σ		$^{238}U/^{206}Pb^*$ date (Ma) ±1σ		$^{207}Pb^*/^{206}Pb^*$ date (Ma) ±1σ		Disc. (%)
I	27	27.1	224	100	0.45	0.019	2.995	0.025	0.11310	0.00057	2.996	0.026	0.11294	0.00058	1857	14	1847	9	-0.5
I	11	11.1	132	53	0.41	0.000	2.976	0.057	0.11311	0.00091	2.976	0.057	0.11311	0.00091	1867	31	1850	14	-0.9
I	24	24.1	738	314	0.43	0.215	2.903	0.038	0.11516	0.00037	2.909	0.038	0.11327	0.00047	1905	22	1853	7	-2.8
I	3	3.1	595	240	0.40	0.080	3.036	0.035	0.11441	0.00038	3.038	0.035	0.11371	0.00041	1834	19	1860	7	1.4
I	8	8.1	586	243	0.42	0.012	3.032	0.035	0.11403	0.00038	3.032	0.035	0.11392	0.00038	1838	19	1863	6	1.4
I	15	15.1	439	360	0.82	0.041	3.074	0.023	0.11431	0.00043	3.076	0.023	0.11395	0.00045	1815	12	1863	7	2.6
I	19	19.1	339	210	0.62	0.040	2.998	0.032	0.11438	0.00049	2.999	0.032	0.11403	0.00051	1855	18	1865	8	0.5
I	26	26.1	497	256	0.51	0.026	2.949	0.028	0.11438	0.00039	2.950	0.028	0.11415	0.00040	1882	16	1867	6	-0.8
I	16	16.1	261	64	0.24	0.040	3.032	0.053	0.11458	0.00054	3.033	0.053	0.11423	0.00056	1837	28	1868	9	1.6
I	17	17.1	224	29	0.13	-0.022	2.905	0.024	0.11416	0.00062	2.904	0.024	0.11435	0.00064	1907	14	1870	10	-2.0
I	1	1.1	339	148	0.44	0.013	2.963	0.022	0.11480	0.00048	2.963	0.022	0.11469	0.00049	1875	12	1875	8	0.0
M	13	13.1	74	37	0.50	0.282	3.098	0.035	0.11109	0.00103	3.107	0.035	0.10864	0.00132	1799	18	1777	22	-1.2
M	10	10.1	440	132	0.30	0.033	2.978	0.023	0.11040	0.00044	2.979	0.023	0.11010	0.00046	1866	13	1801	8	-3.6
M	4	4.1	190	125	0.66	-0.023	3.121	0.026	0.11076	0.00063	3.121	0.026	0.11096	0.00064	1792	13	1815	10	1.3
M	5	5.1	882	236	0.27	0.020	3.074	0.030	0.11142	0.00030	3.074	0.030	0.11124	0.00030	1816	15	1820	5	0.2
M	21	21.1	505	448	0.89	0.005	3.076	0.034	0.11130	0.00041	3.077	0.034	0.11126	0.00041	1814	18	1820	7	0.3
M	12	12.1	139	40	0.29	0.095	3.025	0.062	0.11218	0.00080	3.027	0.062	0.11135	0.00089	1840	33	1822	14	-1.0
M	7	7.1	804	604	0.75	0.017	3.119	0.021	0.11175	0.00031	3.120	0.021	0.11160	0.00032	1792	11	1826	5	1.8
M	6	6.1	363	95	0.26	0.006	3.068	0.023	0.11172	0.00047	3.068	0.023	0.11167	0.00047	1819	12	1827	8	0.5
M	20	20.1	705	567	0.80	0.067	3.205	0.022	0.11229	0.00034	3.207	0.022	0.11171	0.00037	1750	11	1827	6	4.3
M	22	22.1	442	209	0.47	0.101	3.112	0.035	0.11264	0.00043	3.115	0.035	0.11176	0.00048	1795	18	1828	8	1.8
M	14	14.1	297	326	1.10	0.000	3.091	0.048	0.11183	0.00058	3.091	0.048	0.11183	0.00058	1807	24	1829	9	1.2
M	2	2.1	377	212	0.56	0.057	3.143	0.023	0.11234	0.00047	3.145	0.023	0.11184	0.00050	1780	12	1830	8	2.7
M	23	23.1	243	165	0.68	0.010	3.225	0.054	0.11196	0.00060	3.225	0.054	0.11187	0.00060	1741	26	1830	10	4.9
X	9	9.1	889	228	0.26	0.071	2.836	0.028	0.12206	0.00033	2.838	0.028	0.12143	0.00036	1946	17	1977	5	1.6
X	25	25.1	199	72	0.36	0.057	2.718	0.043	0.12978	0.00064	2.720	0.043	0.12927	0.00067	2018	27	2088	9	3.3
D	18	18.1	130	61	0.47	0.116	2.984	0.029	0.10935	0.00080	2.987	0.029	0.10834	0.00090	1861	16	1772	15	-5.1

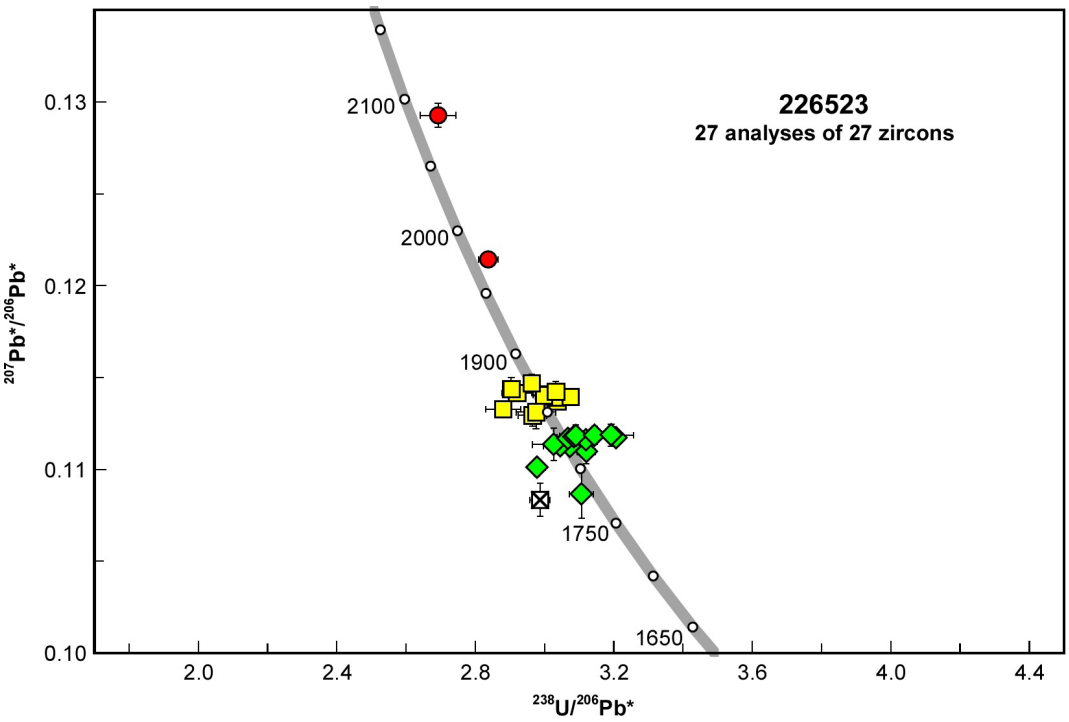

Figure 3. U–Pb analytical data for sample sample 226523: biotite–muscovite granodiorite gneiss, Rose Bore. Yellow squares indicate Group I (magmatic zircons); red circles indicate Group X (xenocrystic zircons); crossed square indicates Group D (discordance >5%)

Interpretation

The analyses are concordant to moderately discordant (Fig. 3). One analysis is >5% discordant. The date obtained from this analysis (Group D; Table 1) is unreliable, and considered not to be geologically significant. The remaining 26 analyses can be divided into three groups, based on their $^{207}Pb^*/^{206}Pb^*$ ratios.

Group I comprises 11 analyses (Table 1), which yield a weighted mean $^{207}Pb^*/^{206}Pb^*$ date of 1863 ± 5 Ma (MSWD = 0.94).

Group M comprises 13 analyses (Table 1), which yield a weighted mean $^{207}Pb^*/^{206}Pb^*$ date of 1822 ± 5 Ma (MSWD = 1.4).

Group X comprises two analyses (Table 1), which yield $^{207}Pb^*/^{206}Pb^*$ dates of c. 2088 and 1977 Ma.

The date of 1863 ± 5 Ma for the 11 analyses in Group I is interpreted as the magmatic crystallization age of the granodiorite protolith. The date of 1822 ± 5 Ma for the 13 analyses in Group M is interpreted as the age of high-grade metamorphism and migmatization. The dates of c. 2088 and 1977 Ma for the two analyses in Group X are interpreted as the ages of xenocrystic zircons.

References

Page, RW and Hoatson, DM 2000, Geochronology of the mafic–ultramafic intrusions, *in* Geology and economic potential of the Palaeoproterozoic layered mafic–ultramafic intrusions in the East Kimberley, Western Australia *edited by* DM Hoatson and DH Blake: Australian Geological Survey Organisation, Bulletin 246, p. 163–172.

Stacey, JS and Kramers, JD 1975, Approximation of terrestrial lead isotope evolution by a two-stage model: Earth and Planetary Science Letters, v. 26, p. 207–221.

Tyler, IM, Hoatson, DM, Griffin, TJ, Sheppard, S, Blake, DH and Warren, RG 1997, McIntosh, WA Sheet 4462: Western Australia Geological Survey, 1:100 000 Geological Series.

Tyler, IM and Phillips, C 2019a, (partial report), Rose Bore Granite (P_-TIrb-mgr): Geological Survey of Western Australia, WA Geology Online, Explanatory Notes extract, viewed 04 December 2019, <www.dmp.wa.gov.au/ens>.

Tyler, IM and Phillips, C 2019b, (partial report), Tickalara Metamorphics (P_-TI-xmw-m): Geological Survey of Western Australia, WA Geology Online, Explanatory Notes extract, viewed 04 December 2019, <www.dmp.wa.gov.au/ens>.

Recommended reference for this publication

Lu, Y, Wingate, MTD and Maidment, DW 2020, 226523: biotite–muscovite granodiorite gneiss, Rose Bore; Geochronology Record 1652: Geological Survey of Western Australia, 4p.

Data obtained: 22 October 2018

Data released: 31 January 2020